Immunobiology 224 (2019) 817–826

Contents lists available at ScienceDirect

Immunobiology

journal homepage: www.elsevier.com/locate/imbio

Effects of intestinal nematode treatment on CD11b activation state in an EAE mouse model of multiple sclerosis

Katarzyna Donskow-Łysoniewska[a,b,*], Katarzyna Krawczak[a], Maja Machcińska[b], Magdalena Głaczyńska[b], Maria Doligalska[a]

[a] Department of Parasitology, Institute of Zoology, Faculty of Biology, University of Warsaw, Warsaw, Poland
[b] Laboratory of Parasitology, General Karol Kaczkowski Military Institute of Hygiene and Epidemiology, Warsaw, Poland

ARTICLE INFO

Keywords:
Parasitic helminths
CD11b integrin
Immunoregulation

ABSTRACT

The experimental autoimmune encephalomyelitis (EAE) animal model of Multiple Sclerosis (MS) is characterized by episodic neurologic dysfunction arising as a consequence of perivascular mononuclear cell infiltration and demyelination in the CNS. Leukocyte integrins, which are responsible for migration through the endothelial, play key roles in the pathogenesis of autoimmune diseases and chronic inflammation. Intestinal infection of mice with *Heligmosomoides polygyrus* appears to target CD11b (integrin αM), which is highly expressed on myeloid cells and is critical for their migration and function. *H. polygyrus* infection induces suppression of ongoing experimental EAE and extensive infiltration of $CD11b^+$ cells to the CNS. Therefore, the aim of the present study was to characterize the phenotype and activity of $CD11b^+$ cells accompanying the tissue phase infection of L4 *H. polygyrus* in EAE mice. It was found that the cells displayed a $CD11b^+$ state with a distinct phenotype characterised by the expression of co-stimulatory CD80/CD86, CD40, MHCII, F4/80 and the mannose receptor CD206. This activation state illustrates the heterogeneity of $CD11b^+$ cells in EAE mice following nematode invasion; these may have important consequences for understanding the effects of CD11b integrin, which is involved in the downregulation of neuroinflammatory disorders.

1. Introduction

Multiple sclerosis (MS) is an autoimmune disease of the CNS characterized by mononuclear cell infiltration and is known to be regulated by autoreactive proinflammatory Th17 and Th1 CD4 T cells; it also follows a similar course to that of experimental autoimmune encephalomyelitis (EAE): an animal model of MS. The subsequent migration and accumulation of the cells in the brain and spinal cord result in elevated levels of cytokines, chemokines, and adhesion molecules, leading to lesion formation, demyelination and the consequent impairment of neuronal transmission (Huitinga et al., 1990; Geurts and Barkhof, 2008). Although activated leukocytes are known to cross the weakened blood-brain barrier (BBB) in EAE (Kawakami et al., 2004; Keating et al., 2009), the molecular mechanisms by which they enter and persist in the CNS remain unclear.

Leukocyte integrins play key roles in the pathogenesis of autoimmune diseases and chronic inflammation. Among the b2 integrins, the most abundant and versatile receptor is macrophage antigen-1 (integrin Mac-1, αMβ2, CD11b/CD18) (Abram and Lowell, 2009), also known as complement receptor 3 (CR3). Ligand engagement by Mac-1 initiates a variety of leukocyte responses, including adhesion, migration through endothelial cells, phagocytosis and degranulation (Springer and Anderson, 1986). Its activity mediates adhesion to C3bi and ICAM-1/CD54 is formed by CD11b (Integrin αM/ITGAM) which combines with integrin β2 (CD18).

Although the integrin CD11b is one of the most intensively-studied leukocyte adhesion factors (Liu and Kubes, 2003), its relative contribution in the development of CNS demyelinating diseases is poorly understood and published findings are contradictory. While homozygous mice deficient in $CD11b^+$ cells displayed attenuated EAE with a significantly delayed onset (Bullard et al., 2005), the presence of CD11b on antigen-presenting cells plays a critical role in promoting oral tolerance in some autoimmune disorders (Ehirchiou et al., 2007) and has been proposed as an important target for MS immunotherapy (Bullard et al., 2005).

Considering the capacity of helminths to induce anti-inflammatory immune responses (Sewell et al., 2003a; La Flamme et al., 2003; Zheng et al., 2008; Terrazas et al., 2017), the therapeutic efficacy of the intestinal nematode *Heligmosomoides polygyrus* in ongoing EAE in mice was found to be connected with an increased number of CD11b cells at

* Corresponding author. Present address: Laboratory of Parasitology, General Karol Kaczkowski Military Institute of Hygiene and Epidemiology, Warsaw, Poland.
E-mail address: katarzyna.d.lysoniewska@wihe.Pl (K. Donskow-Łysoniewska).

https://doi.org/10.1016/j.imbio.2019.08.004
Received 24 March 2019; Received in revised form 7 June 2019; Accepted 10 August 2019
Available online 13 August 2019

the early prepatent phase (Donskow-Łysoniewska et al., 2017). Although *H. polygyrus* is known to display immune modulating activity, inhibition of disease, as described by clinical score and reduced demyelination, was typically observed six days post infection, i.e. when L4 stage had become localized in the small intestine wall (Donskow-Łysoniewska et al., 2012, 2017). Therefore, this is an excellent time period to study the mechanisms involved in reducing inflammation in the CNS by examining the immune status and cells involved in the inhibition of EAE in mice. EAE inhibition occurred despite a significant reduction in the number of nematodes in the intestine; in addition, attenuated clinical signs were not associated with the absence of immune cell infiltrates in the CNS, but with extensive infiltration of various regulatory leukocytes including $CD11b^+$ mononuclear cells (Donskow-Łysoniewska et al., 2017).

The relative contribution of $CD11b^+$ cells to the progression of EAE remains unknown, as does its inhibition. Despite its side effects, therapy with live nematodes (helminth therapy) can offer an insight into the pathological and or immunomodulatory processes responsible for neurodegenerative diseases, and may facilitate the development of new strategies for biological therapies. Therefore, to better understand the related immunomodulatory mechanisms, there is a clear need to identify the components of the immune system that are activated by helminthic antigens.

The present study examines the effect of *H. polygyrus* infection on the expression of antigen-presenting molecules, adhesion molecules and costimulatory molecules on CD11b cells. It also evaluates the activity of these cells in the peritoneal cavity and the cerebrospinal fluid of mice with EAE according to the knowledge that majority of brain phagocytes found after lesions originate from invading cells. Together with other recent reports, these findings may better clarify the role of CD11b cells, including neutrophils, in regulating inflammation in neurodegenerative disorders, thus creating the basis for new therapeutic approaches.

2. Material and methods

2.1. Ethics statement

All experiments were conducted according to the Polish Law on Animal Experimentation and EU Directive 2010/63/UE, and approved by the First Warsaw Local Ethics Committee (ID 151/2011).

2.2. Schedule of the experiment

The experiments were conducted on eight-week-old, pathogen-free female C57BL/6 mice. The mice weighed 20–25 g at the start of the study, and were kept in standard light:dark conditions (12 h/12 h) at a temperature of 24–25 °C with *ad libitum* access to water and commercial pellet food. All mice were allowed to adjust to laboratory conditions for a minimum of seven days before experimental manipulation. All experiments included a number of groups: an uninfected control group (CTR), an immunized group (EAE), an immunized group infected with *H. polygyrus* (EAE/Hpoly) and a group only infected with *H. polygyrus* (Hpoly). Each experimental group consisted of six animals kept together in one cage.

2.2.1. Induction of EAE and nematode infection

Mice were injected s.c. into the rear flanks on day 0 with 100 µl of 200 µg of myelin oligodendrocyte glycoprotein MOG_{35-55} (purity > 95%) emulsified in complete Freund's adjuvant (CFA) containing 300 µg *Mycobacterium tuberculosis* H37RA strain. Immediately thereafter, and again 48 h later, the mice received an intraperitoneal injection of 400 ng of *Bordetella pertussis* toxin (PTX; Sigma, St. Louis, MO, USA) in 100 µl of PBS; pH 7.2.

The mice were weighed and were scored daily according to the following criteria: 0, normal; 1, limp tail; 2, hind limb weakness; 3, partial hind-limb paralysis; 4, complete hind-limb paralysis; 5, hind-limb and forelimb paralysis.

Twenty-one days post-immunization, the animals were infected *per os* with *H. polygyrus* 300 L3 stage (EAE/H poly group) or treated with water (EAE group) and studied at the sixth day post infection (DPI).

2.3. Cerebrospinal fluid and peritoneal fluid collection

Cerebral spinal fluid (CSF) was collected as previously described (Donskow-Łysoniewska et al., 2017). Peritoneal cavity fluids (PF) were collected from mice by injection of 5 mL of RPMI 1640 medium supplemented with penicillin/streptomycin (100 µg/ml) and 2 mM L-glutamine (Gibco UK). The PF were collected separately and centrifuged at 1200 rpm at 4 °C for 15 min. The cells were counted using a Muse Count and Viability Assay kit (Merck Millipore, USA) followed by a Muse Cell Analyzer (Merck Millipore, USA) in accordance with the manufacturer's instructions and recovered for cellular analysis or cell culture depending on the experiment.

2.4. Flow cytometric analysis

The PF and CSF cells were used for flow cytometry. For the detection of macrophage-associated surface markers, the following fluorochrome-conjugated monoclonal antibodies were used: CD11b-PercP-Cy5.5, F4/80-FITC or –PE, CD80-APC, CD86-PeCy-7, MHCI-PE, MHCII-FITC, Mannose receptor (MR, CD206)-Alexa488, CD40-PerCP e-Fluor 710 (all from BD Biosciences, Pharmingen, San Diego, CA, USA). Isotype matched Ig control were used to assess the background staining. All antibodies were used according to the manufacturers' protocols and flow cytometry analysis was performed according to the standard protocol. Briefly, the cells (1×10^6) were washed with PBS and incubated with monoclonal antibodies for 30 min at 4 °C. Following this, flow cytometry analysis was performed with FACSVerse using FACSuite software (Becton Dickinson). Compensation was adjusted using BD CaliBRITE Beads (BD Bioscience). The FACS profile and gating strategy are presented in Figs. 2 and 3. A viable acquisition list gate was established using forward and side light scatter (FSC, SSC) parameters to exclude subcellular debris and multi-event clusters.

Two or three-colour fluorescence flow cytometry analysis was performed. The expression of detected markers was estimated as mean fluorescence intensity (MFI). Although lymphocytes are excluded in the initial gating strategy, no specific dendritic cell and neutrophil markers were investigated to discriminate these cells and then they might be present in a limited percentage in the $CD11b^+$ mixed population.

2.5. Measurement of $CD11b^+$ cell activity

$CD11b^+$ cells were isolated from the CSF and PF of the mice using EasySep®Magnetic Mouse Monocyte Enrichment Kit (Stemcell Technologies Inc., Vancouver, BC) according to the manufacturer's instructions. The flow cytometry results found the monocyte content ($CD11b\text{-}PercP\text{-}Cy5.5^+$) to be 96% for PF and 95.8% for CSF. Freshly isolated cells were examined for reactive oxygen species (ROS) concentration, nitric oxide (NO) concentration, mixed lymphocyte reactions and levels of synthase iNOS, chitinase-3-like protein-3 Ym-1 and arginase-1 Arg-1 transcripts.

2.6. Quantification of NO and ROS

For activity measurement, $2{\cdot}10^5$ PF and CSF isolated $CD11b^+$ cells were incubated at 37^0C and 5% CO_2 in RPMI1640 supplemented with 100 U/ml penicillin/ streptomycin (Gibco, Inchinnan, Scotland, UK). After 48 h of incubation with LPS (2 µg/ml) or $MOG_{35\text{-}55}$ (5 µM), the supernatants were harvested for nitrite measurement, and the cells were collected by 30-minute incubation with Accutase (eBioscience Inc., San Diego, USA) for ROS measurement. The supernatants were assayed for nitrate/nitrite using a commercially-available colorimetric

assay kit (Nitrate/Nitrite Colorimetric Assay Kit Cayman Chemical Company, Michigan, USA). Assays were performed according to the manufacturer's protocol. The results were presented as Nitrate (NO_3) + Nitrite (NO_2) (μM).

The Muse™ Oxidative Stress kit (Merck Millipore) was used to estimate the relative percentages of ROS-negative and ROS-positive $CD11b^+$ cells (2·105). The gating strategy is presented in Fig. 4D. All procedures were performed according to the manufacturer's guidelines.

2.7. Quantification of iNOS, Ym-1 and 1 Arg-1 transcript level

RNA from *ex vivo* collected $CD11b^+$ cells was extracted using the SV Total RNA Isolation System (Promega, Madison, USA) according to the manufacturer's instructions. Approximately 20 ng of RNA was used as a template for cDNA synthesis, performed using a first-strand cDNA synthesis kit (Thermo Scientific, Epsom, Surrey, UK) with TaqMan Gene Expression Assays. Fragments of the *Mus musculus iNos, Arg-1, Ym1* and GAPDH (housekeeping gene) cDNA were amplified by PCR using the following primer sets: *iNos*2 (Mm00440502_m1), *Arg1* (Mm00475988_m1), *Ym1* (Mm00657889_mH) and *Gapdh* (Mm00440502_m1).

The reactions contained cDNA (20 ng), master mix containing polymerase (Thermo Scientific Luminaris Color Probe High ROX qPCR Master Mix Thermo Scientific Inc.) and 0.5 mM of each gene-specific primer. PCR was performed on a Quantica thermocycler (Techne, Staffordshire, UK) using the two-step cycling protocol according to the manufacturer's instructions. Transcript level quantification was performed by Quantica software. Results from each sample were averaged and normalized to the mean GAPDH level to control for variability in cDNA amount and reaction efficiencies.

2.8. $CD11b^+$ cells effect on CD4 T cell proliferation

To determine the proliferative effects of the isolated $CD11b^+$ cells of EAE/Hpoly mice on purified $CD4^+$ T-cells *ex vivo*, mixed leukocyte reactions (MLR) were performed.

For negative selection of $CD4^+$ T-cells from CSF and PF, 1×10^6 MLN cells were incubated with a 10 μl mix of antibodies against surface antigens to non-$CD4^+$ T cells for 15 min at 4 °C in PBS/1% BSA and enriched by magnetic field-assisted cell sorting (Dynal Mouse CD4 Negative Isolation Kit, Invitrogen). Following this, co-cultures were created by adding 1.25×10^4 $CD11b^+$ isolated from the EAE/Hp or EAE mice in 50 μl media to 5×10^4 EAE lymphocytes in 50 μl media.

The mixture was incubated for 48 h at 37 °C and 5% CO_2 with 5 μM of $MOG_{35–55}$ in 96-well flat bottom plates (Costar, Cambridge, MA) and then cell proliferation was evaluated. Optimal cell proliferation was observed at a $CD11b^+$: T cell ratio of 1:4, as determined in a preliminary study. Controls were set without addition of $CD11b^+$ cells.

After 48 h of culture, proliferation was evaluated using the MTS colorimetric method (Cell Titer 96® Aqueous One Solution Cell Proliferation Assay, Promega, USA) (Donskow-Łysoniewska et al., 2017). Absorbance was measured at 490 nm in a plate spectrophotometric reader (u-Quant, BD, Costar, Acton MA, USA). The proliferation of lymphocytes was presented as optical density (OD).

2.9. Immunohistological analysis

Brain sections 8 μm thick were prepared (Donskow-Łysoniewska et al., 2017) and stained with CD206 Monoclonal Antibody (MR5D3, Invitrogen) and secondary antibody Alexa Fluor 594 rabbit anti-rat IgG (H + L). Nuclei were stained with DAPI (4′, 6-diamidino-2-phenylindole, Biostatus, Shepshed, UK), and sections were visualized using a Fluorescence Microscopy Nikon Eclipse (Nikon Instruments Inc, Melville, NY, USA). To quantify the numerical densities of cells positive for staining with anti-CD206 mAb and DAPI in brain tissue, images of each section were analysed in the NIS Elements BR 4.4 Program (Nikon, Tokyo, Japan).

2.10. Statistical analyses

Groups of six mice were used in each independent experiment, and each experiment was performed in triplicate yielding similar results. Results were analysed using analysis of variance (ANOVA) by MINITAB Software (Minitab Inc., PA, USA). Differences between groups were considered significant when P value < 0.05. The representative results of one experiment are presented. Data is presented as the mean ± SD.

3. Results

3.1. The influence of H. polygyrus larvae on the severity of ongoing EAE

The disease incidence was 100% among the C57BL/6 females injected with $MOG_{35–55}$. Development of EAE was observed from seven days post immunization, and the disease peaked at 21 days. The control mice injected with PBS did not develop any clinical symptoms. From the second day of infection, significant inhibition of disease was observed in the mice treated with *H. polygyrus* compared to PBS-treated EAE mice. Minimal symptoms of the disease was observed in 100% of mice at 6 DPI (Fig. 1).

3.2. Changes in the peritoneal and cerebrospinal cell population

On day 6, infection with stage L4 was associated with a decrease in total leukocyte number in the PF but an increase in total leukocyte number in the CSF (Tables 1 and 2). To determine the type of $CD11b^+$ cell activation by the nematode, the expression of major histocompatibility complex (MHC) class II, MHC class I, CD80 and CD86, F4/80, CD40 and CD206 mannose receptor was measured. In the mice treated with EAE, nematode treatment was associated with an increase in the percentage of total $CD11b^+$ cells in the CSF, with the number being slightly higher than in the PF. In the peritoneal cavity, $CD11b^+$ cells were recognized as $CD11b^{hi}$ and $CD11b^{lo}$ (Table 1, Fig. 2A). Following infection with the nematode, the percentage of $CD11b^{lo}$ cells fell from approximately 70% to 25%; however, the percentage of $CD11b^{hi}$ rose from 25% to over 71% of total $CD11b^+$ cells (Table 1). No $CD11b^{hi}$ or $CD11b^{lo}$ divisions were observed in the CSF (Fig. 3A).

Exposure to nematode infection modified the surface markers of the $CD11b^+$ cells of both the PF and the CSF (Tables 1 and 2; Figs. 2 and 3). In EAE mice, the $CD11b^{hi}$ cells of the PF were initially positive for MHCI, CD80, CD86, CD40, F4/80 and MMR, and nematode infection increased the percentage of MHCII and MMR in F4/80-positive $CD11b^{hi}$ cells. Nematode infection also increased the expression of MHCII and CD80 on the $CD11b^+$ cells.

The main phenotypic changes were related to the $CD11b^{lo}$ PF division. Nematode exposure reduced the number of $CD11b^{lo}$ in the peritoneal cavity; in addition, the percentage of cells expressing MHCII, CD86, F4/80 and MMR, and MFI excluding MMR, was increased (Table 1), while the percentage of $CD80^+$ and $CD40^+$ $CD11b^{lo}$ cells decreased. The percentage of $CD11b^{lo}$ that was negative for F4/80 or MMR was also increased.

In the PF, the expression of CD206 (MMR) was found to change significantly on $CD11b^+F4/80^+$ cells following nematode treatment; in addition, among the cells expressing F4/80 and MMR, the percentage share of total CD11b and $CD11b^{lo}$ decreased while $CD11b^{hi}$ increased. In contrast, in the CSF, the proportion of $CD11b^+$ cells expressing F4/80, including MMR^+ cells, decreased; in addition, the $CD11b^+$ cells in both infected and uninfected EAE mice were found to be positive for MHCI, CD80 and CD86; nematode exposure increased the MHCII population, but decreased the MMR^+ and $CD40^+$ $CD11b^+$ populations.

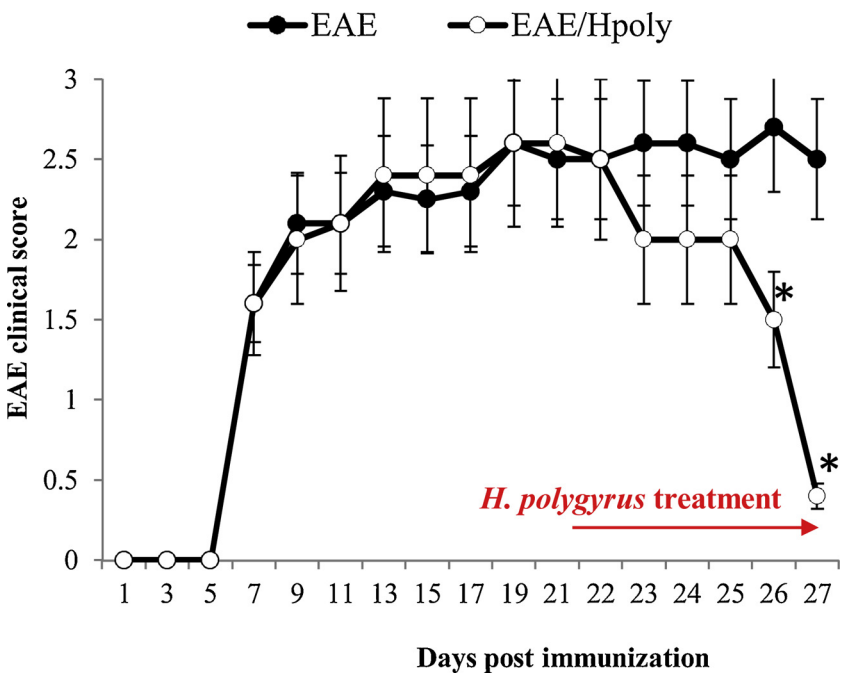

Fig. 1. Infection with *H. polygyrus* ameliorates the clinical signs and disease progression of MOG- induced EAE. C57BL/6 females were immunized with MOG_{35-55}-peptide in CFA containing *M. tuberculosis* H37RA strain and pertussis toxin to induce EAE. L3 stage *H. polygyrus* was orally administered at day 21 post immunization. Mice were weighed and clinically scored daily. One representative experiment is presented as the mean ± SD of six mice per group. $^{*}p < 0.05$ compared with the EAE group at the same day (ANOVA).

3.3. Activity of $CD11b^+$ cells

As nematode infection influenced the phenotype of CD11b cells in EAE mice, the next part of the study examined the impact of infection on the expression of synthase iNOS, chitinase-like protein (Ym1) and arginase-1 (Arg1), as well as on NO production and reactive oxygen species (ROS) concentration (Fig. 4).

The expression of iNOS2 was significantly reduced in EAE mice infected with nematodes at 6 DPI, while the expression of Ym1 was slightly increased. Nematode treatment significantly enhanced arginase-1 expression in the PF cells but inhibited it in the CSF cells (Fig. 4A). The nitrate/nitrite activity reflected iNOS gene expression (Fig. 4B); however, while nematode infection significantly reduced the percentage of ROS^+ macrophages by approximately half to 22% in the PF, no such significant effect was observed for CD11b cells in the CSF (Fig. 4C).

3.4. T cell activation

Stimulator cells- $CD11b^+$ of EAE/Hpoly group influence were evaluated. MLR in response to $CD11b^+$ of EAE mice was served as control. To determine whether the peritoneal and cerebrospinal CD11b cells from infected animals retained their antiproliferation ability, the $CD11b^+$ cells and CD4+ lymphocytes were co-cultured. The profiles of the CSF and PF of infected mice with EAE indicated that the co-cultured cells had anti-proliferative effects on $CD4^+$ T cells (Fig. 5). The CSF $CD11b^+$ cell population isolated from nematode-infected EAE mice was able to suppress encephalitogenic T cell proliferation to $MOG_{35–55}$ by 62%. The antiproliferative effects were not caused by increased apoptosis of the lymphocytes. All cell cultures demonstrated comparable high viability (> 98%).

3.5. Mannose receptor expression CD206

To characterize the mannose receptor $CD206^+$ cells in the brain, immunofluorescent staining was performed with antibodies for CD206 on $DAPI^+$ cells (Fig. 6). A significant difference was found between uninfected and infected EAE mice with regard to the numbers of $CD206^+/DAPI^+$ cells per section (Fig. 6A). The sections taken from infected EAE mice demonstrated strong staining for $CD206^+$ cells and greater numbers and percentages of $CD206^+/DAPI^+$ cells (Fig. 6B,C).

4. Discussion

Leukocyte accumulation is a key feature of chronic inflammation associated with neurodegeneration. However, the mechanisms underlying leukocyte accumulation in CNS tissue and the precise functions of different leukocyte phenotypes have yet to be defined.

CD11b integrin is a well-known regulator of leukocyte migration and adhesion (Abram and Lowell, 2009, Springer and Anderson, 1986). Our previous study revealed that following nematode induction, CD11b could play an important role in mediating the influx of monocyte myeloid lineage cells to the CNS during MOG- induced EAE (Donskow-Łysoniewska et al., 2017). Pro-inflammatory immune responses are central to the development of ongoing autoimmunity in EAE, and it has been hypothesized that their inhibition following treatment with intestinal nematodes may be connected with the traffic of induced regulatory cells from the periphery to the site of autoimmunity; this movement may prevent tissue destruction and/or induced neuroregeneration and/or neuroprotection (Ghosn et al., 2010). However, our previous results indicate that the improvements in EAE observed in model mice occur as a synergistic effect of the enhanced migration of different regulatory cell populations following peripheral induction; in this scenario, it is likely that the promotion of alternative activation is key to developing the phenotype characterised by $CD11b^+$ leukocytes.

Although helminth infection has been proposed to govern the migration of macrophages into the inflamed CNS during EAE (La Flamme et al., 2003; Zheng et al., 2008; Terrazas et al., 2017), a little is also known of the regulation of cell infiltration and extravasation from sites of inflammation associated with nematode- induced abrogation of ongoing autoimmune disease. Typically, during infection, the activity of Th2 cytokines promotes the local proliferation of macrophages with an alternative activation phenotype. The ratio of M1-like/M2-like macrophages is highly regulated under physiological and pathological conditions; however, it decreases during the infection process, as monocytes in the peripheral tissue may differentiate into final macrophages not simply restricted to a single activation state. Macrophages in various tissues can be maintained autonomously, and their precursors may not be derived from bone marrow. In some tissues, macrophages are able to self-renew and proliferate locally in a static state (Ajami et al.,

Table 1
The influence of L4 stage *H. polygyrus* on the peritoneal cavity cell response of EAE mice six days after infection. The table presents I. the total number of peritoneal cavity cells analyzed with a Muse Cell Analyzer; II. the percentage and the mean fluorescence intensity (MFI) of CD11b$^+$ cells positively expressing surface markers identified by FACS. *$p < 0.05$ compared with EAE group (ANOVA).

Peritoneal cavity	EAE	EAE/Hpoly
Number of leukocytes (x 10^3/μl)	30,00 ± 3,56	6,80 ± 1,06*
Percentage (%)		
Total CD11b$^+$	96,38 ± 3,11	86.89 ± 8,74
MHCII$^+$	26,40 ± 2,95	87,69 ± 3,09*
MHCI$^+$	99,25 ± 0,72	99,17 ± 0,67
CD80$^+$	80,36 ± 1,02	87,96 ± 7,67
CD86$^+$	36,65 ± 3,36	78,81 ± 5,47*
F4/80$^+$	78,66 ± 3,17	90,44 ± 5,62
CD40$^+$	81,23 ± 4,08	24,76 ± 1,37*
MMR$^+$	87,81 ± 8,97	97,24 ± 1,16
MMR in CD11b$^+$ F4/80$^+$	22,08 ± 1,9	14,23 ± 1,10*
CD11b^{hi}	25,96 ± 4,92	71,07 ± 3,81*
MHCII$^+$	65,47 ± 6,92	98,63 ± 1,17
MHCI$^+$	99,83 ± 0,20	99,77 ± 0,12
CD80$^+$	99,61 ± 0,32	99,64 ± 0,12
CD86$^+$	98,22 ± 1,56	94,65 ± 1,95
CD40$^+$	99,15 ± 0,39	98,99 ± 1,02
F4/80$^+$	99,30 ± 0,22	99,77 ± 0,82
MMR$^+$	99,48 ± 0,43	99,93 ± 0,12
MMR in CD11b$^+$ F4/80$^+$	59,40 ± 5,99	76,40 ± 5,34*
CD11b^{lo}	70,42 ± 2,46	15,82 ± 2,22*
MHCII$^+$	8,08 ± 1,61	54,49 ± 6,74*
MHCI$^+$	99,06 ± 1,14	98,72 ± 1,73
CD80$^+$	72,59 ± 3,32	54,47 ± 1,85*
CD86$^+$	44,21 ± 5,3	85,25 ± 2,61*
F4/80$^+$	62,03 ± 4,61	89,18 ± 2,39*
CD40$^+$	65,79 ± 1,00	11,25 ± 0,62*
MMR$^+$	79,90 ± 8,17	97,05 ± 1,61*
MMR in CD11b$^+$ F4/80$^+$	51,38 ± 1,35	7,08 ± 0,65*
MFI		
Total CD11b$^+$	7305 ± 197,09	22058 ± 527,51*
MHCII$^+$	6439 ± 464,11	21240 ± 1073,02*
MHCI$^+$	7658 ± 515,93	21916 ± 2879,12*
CD80$^+$	1413 ± 173,22	6889 ± 182,19*
CD86$^+$	7618 ± 320,30	6835 ± 1000,10
CD40$^+$	5678 ± 860,65	10987 ± 254,16*
F4/80$^+$	19117 ± 1217,30	6686 ± 876,38*
MMR$^+$	963 ± 57,46	1630 ± 87,30*
CD11b^{hi}	47711 ± 1634,40	41836 ± 537,43
MHCII$^+$	5084 ± 230,16	20004 ± 1344,53*
MHCI$^+$	25172 ± 2110,11	26104 ± 2138,89
CD80$^+$	4355 ± 116,82	8399 ± 6294,96*
CD86$^+$	12349 ± 458,08	7645 ± 250,43*
CD40$^+$	7896 ± 669,75	5231 ± 239,76
F4/80$^+$	40132 ± 3186,47	32637 ± 1625,66
MMR$^+$	1176 ± 71,08	1630 ± 38,43
CD11b$^+$lo	365 ± 35,68	3668 ± 183,09*
MHCII$^+$	20880 ± 593,59	30483 ± 2306,42*
MHCI$^+$	4895 ± 157,87	13493 ± 1871,48*
CD80$^+$	804 ± 7,21	2513 ± 227,17*
CD86$^+$	927 ± 70,06	1216 ± 258,57*
CD40$^+$	3098 ± 49,42	3982 ± 253,76
F4/80$^+$	6637 ± 230,34	4156 ± 57,03*
MMR$^+$	987 ± 38,51	243 ± 52,05*

Table 2
The influence of L4 stage *H. polygyrus* on the cerebrospinal fluid cell response of EAE mice six days after infection. The table presents I. the total number of peritoneal cavity cells analysed with a Muse Cell Analyzer; II. the percentage and the mean fluorescence intensity (MFI)of CD11b$^+$ cells positively expressing surface markers identified by FACS. *$p < 0.05$ compared with EAE group (ANOVA).

Cerebrospinal fluid	EAE	EAE/Hpoly
Number of leukocytes (x 10^3/μl)	6,4 ± 0,47	11,7 ± *0,68
Percentage (%)		
Total CD11b$^+$	1,18 ± 0,27	3,43 ± 0,36*
MHCII$^+$	48,00 ± 3,77	60,79 ± 1,95*
MHCI$^+$	93,47 ± 1,18	94,68 ± 1,51
CD80$^+$	94,00 ± 1,53	90,45 ± 0,59
CD86$^+$	97,47 ± 0,92	91,55 ± 1,14
CD40$^+$	13,44 ± 1,96	6,83 ± 1,09*
F4/80$^+$	49,32 ± 2,93	33,93 ± 1,42*
MMR$^+$	48,31 ± 2,75	32,52 ± 1,72*
F4/80+/MMR	51,71 ± 0,88	33,80 ± 0,81*
MFI		
Total CD11b$^+$	1179 ± 85,13	2017 ± 245,05
MHCII$^+$	6409 ± 81,54	5636 ± 328,32
MHCI$^+$	3683 ± 274,81	6933 ± 211,34
CD80$^+$	951 ± 112,33	1568 ± 76,96*
CD86$^+$	927 ± 81,07	644 ± 65,11
CD40$^+$	1624 ± 63,02	1786 ± 95,60
F4/80$^+$	2285 ± 109,83	2338 ± 237,27
MMR$^+$	5752 ± 223,93	4355 ± 136,27

2007) and in low-grade and chronic inflammation, typical of autoimmune diseases, macrophage accumulation is probably determined by local proliferation (Robbins et al., 2013).

When in the small intestine, the nematode is capable of recruiting immune cells with potent suppressor activity to the peritoneal cavity (Ghosn et al., 2010). Based on our previous findings (Donskow-Łysoniewska et al., 2017), and to avoid the limitations associated with the expression of CD11b markers on microglia (Ponomarev et al., 2005), the present study used CSF to determine the phenotype of the CD11b cells in the CNS of the infected mice, as this fluid is representative of the immune status of the CNS (Renno et al., 1994). Further, to determine the phenotype of the CD11b$^+$ cells in ongoing EAE following *H. polygyrus* nematode infection, the expression of various associated markers on these leukocytes was measured on day six of infection, these being isolated locally from the peritoneal cavity and in targeted tissue (i.e. from the CSF and the brain).

Our findings demonstrate that nematode infection produces an almost fivefold reduction in the number of CD11b$^+$ cells induced in the peritoneal cavity and greatly increases their accumulation in the CSF. In addition, the cells found in the PF and CSF are heterogeneous in terms of surface marker expression. The influx of cell populations into the peritoneal cavity in the EAE mice following intestinal nematode infection consists of two distinct populations based on the expression of the CD11b cell surface marker.

In the PF, the number of leukocytes drastically decreased after nematode infection, and within the total CD11b$^+$ population, the proportion of CD11b^{lo} was shifted in favour of CD11b^{hi}. In infected mice, the percentage of CD11b^{hi} and CD11b^{lo} cells expressing MHC class II molecules was found to be enhanced and the percentage of the CD11b$^+$ cell population co-expressing CD206 (MMR) indicated the presence of alternatively-activated cells (Matsushima et al., 2013). Indeed, the percentage of MMR$^+$ CD11b cells in CD11b^{hi} remained high, and was even found to increase in CD11b^{lo}, resulting in an overall increase of CD11b$^+$ cell numbers. The presence of alternatively-activated cells was also indicated by a greater percentage of CD11b^{hi}F4/80$^+$ cells co-expressing MMR; however, a smaller proportion of CD11b^{lo} F4/80$^+$ cells also expressed MMR. Interestingly, the CD11b^{hi} population predominated in the PF samples, and although their proportion did not appear to be influenced by nematode exposure, their expression of MHC class I, CD80 and CD86, and the percentage of those expressing CD11b^{lo} was modified.

The phenotype of the CD11b population in the CSF corresponded to the CD11b^{hi} population identified in the PF, showing high expression of MHC class I, CD80 and CD86 markers. The percentage of CD11b$^+$ MHCII$^+$ cells increased, but the expression of the MHCII receptor was unaffected; in addition, while the expression of MHCI and

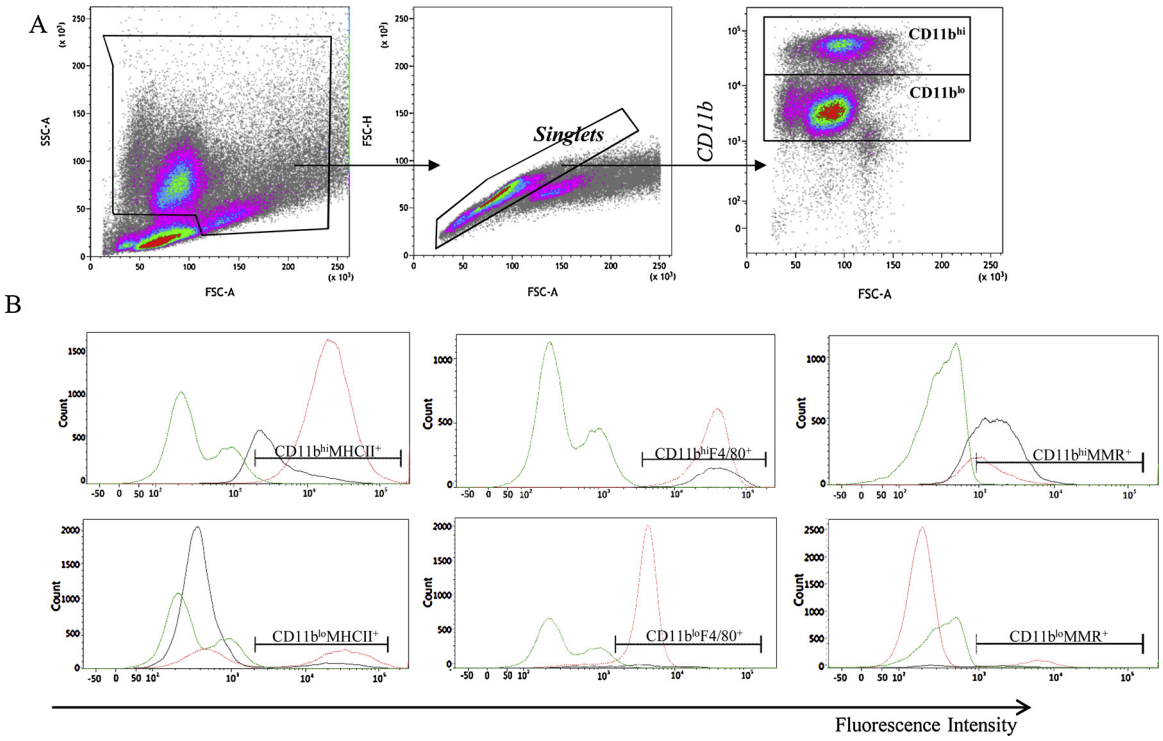

Fig. 2. The effect of *H. polygyrus* infection on receptor expression on CD11b$^+$ cells in the peritoneal cavity in EAE mice at six days post infection. (A) Gating strategy used to identify CD11b$^+$ cell subsets in the peritoneal fluid cavity. Excluding lymphocytes, leukocytes population was gated based on morphological parameters on a forward vs side scatter (FSC/SSC) plot (P1) and further characterized based on their expression of the CD11b receptor in the doublet exclusion gate (P2). A representative FACS plot showing CD11b^{hi} and CD11b^{lo} cells (B). Surface expression of MHCII, F4/80 and MMR staining on CD11b^{hi} and CD11b^{lo} cells. FACS histograms were obtained by gating cells based on positive CD11b staining: black solid line- EAE immunized mice, red dot line- EAE immunized mice treated with *H. polygyrus*, green dash line- unlabelled cells. The experiment shown is representative of three others with similar outcomes. (For interpretation of the references to colour in this figure legend, the reader is referred to the web version of this article).

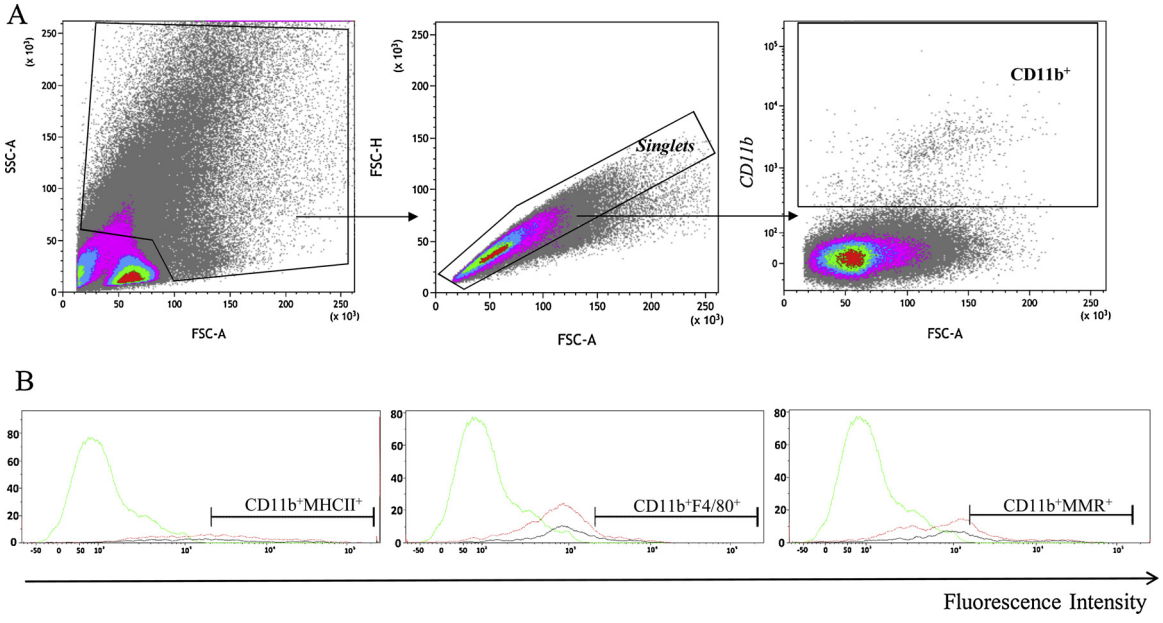

Fig. 3. The effect of *H. polygyrus*infection on the expression of receptors on CD11b$^+$ cells in the cerebrospinal fluid in EAE mice at six days post infection. (A) An analysis of cerebrospinal leukocyte subsets. Excluding lymphocytes, leukocytes population was gated based on morphological parameters on a forward vs side scatter (FSC/SSC) plot (P1) and further characterized according to their expression of the CD11b receptor in the doublet exclusion gate (P2). (B) Surface expression of MHCII, F4/80 and MMR staining on CD11b$^+$ cells. FACS histograms were obtained by gating cells based on positive CD11b staining: black solid line- EAE immunized mice, red dot line- EAE immunized mice treated with *H. polygyrus*, green dash line- unlabelled cells. The experiment shown is representative of three others with similar outcomes. (For interpretation of the references to colour in this figure legend, the reader is referred to the web version of this article).

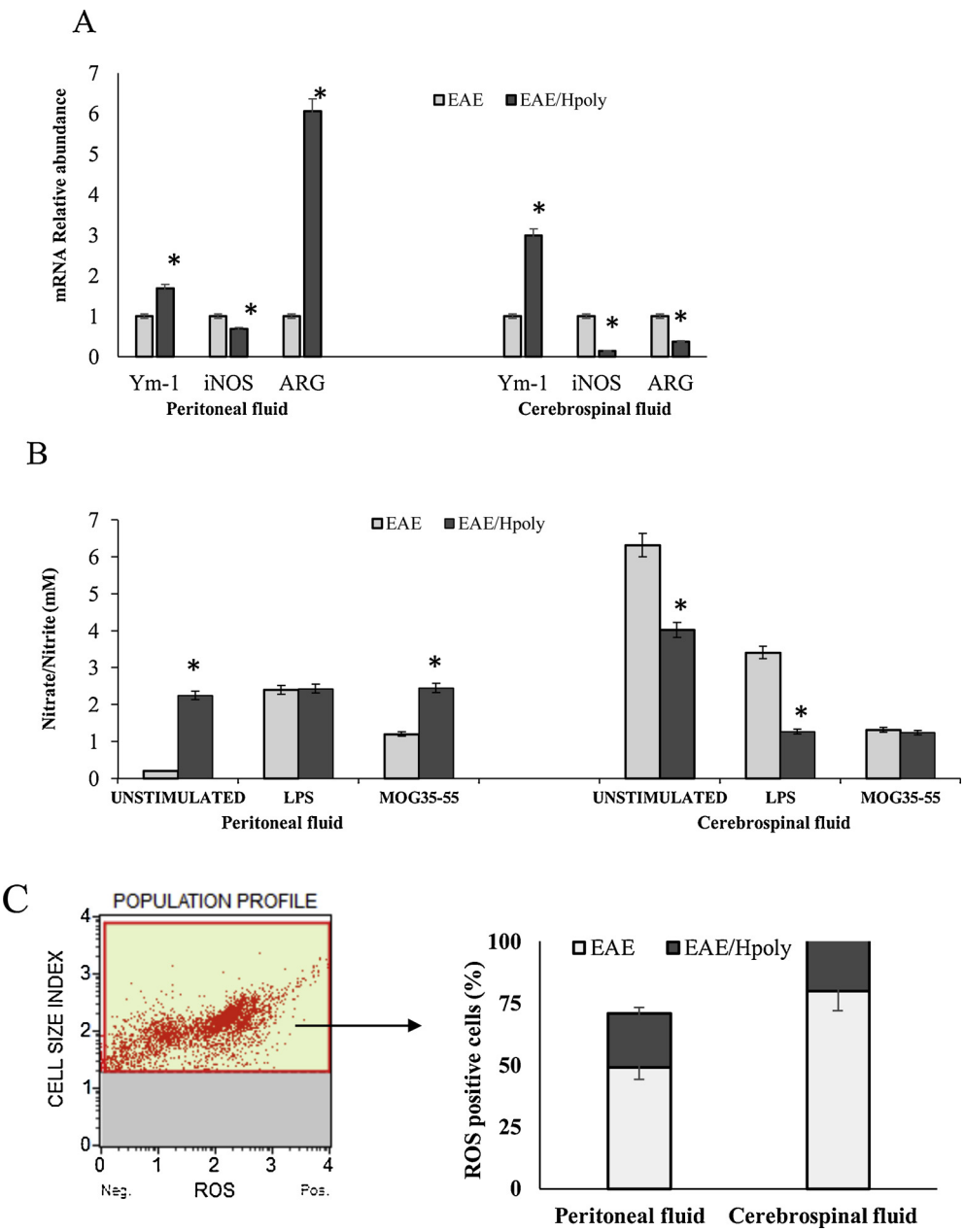

Fig. 4. Polarization of CSF CD11b$^+$ cells in EAE mice infected with *H. polygyrus* at day six of infection. The levels of *Ym1, iNOS and Arg-1* gene expression were determined with quantitative PCR and presented as copy numbers within GAPDH copies (A). Nitrate/Nitrite production in cells stimulated with LPS and MOG_{35-55} peptide (B). ROS production in cells (C). ROS was estimated with The Muse® Oxidative Stress Kit by Muse Cell Analyzer. Gating of CD11b$^+$ cells for superoxide analysis. The mean ± SD of target gene expression was calculated from three independent biological replicates. Results are presented as means ± SD of one representative experiment (n = six mice per group). * indicates a significant relationship between the infected and uninfected EAE groups at $p < 0.05$ (one-way ANOVA).

costimulatory CD80 molecules increased, no such change was observed for CD86. The peritoneal cavity is predominantly composed of macrophages and can be the main source of the partly-definite phenotype that was found to migrate to the CNS in EAE mice following nematode treatment. Decreased expression of CD80 on macrophages, and a blockade of CD80 and CD40 has been reported to suppress EAE (Dudhgaonkar et al., 2009). In the present study, nematode infection significantly decreased the number of CD11b cells expressing CD40 in both the PF and CSF.

One of the earliest events taking place following Ag uptake and activation by APC is the up-regulation of the costimulatory markers CD80 and CD86, as well as that of various activation markers such as MHCII and CD40 Ag on the cell surface. These co-stimulatory molecules are involved in regulating and maintaining the interaction between macrophages and T cells (Kawakami et al., 2004). Our present findings indicate the presence of a low level of encephalitic T cell activation *in vitro* following provocation by CD11b$^+$ cells with high MHCII and CD80 expression and low CD40 expression; this suggests that the nematode may influence the presentation of antigens to T cells by antigen-specific receptors (TCR), with molecular interactions such as CD40L:CD40 being impaired. CD40/CD40L signalling has been shown to play a critical role for the induction of EAE in the absence of CD28-mediated co-stimulation (Girvin et al., 2002). However, despite the abundant expression of costimulatory molecules such as CD80, certain differentiated APCs can be fully capable of suppressing T cell activation (Akbari et al., 2001). Further studies are required using models of mouse EAE with the CD40 blocked in APCs to determine the role played by CD40/CD40L signalling in the relationship between nematode application and disease resistance, and to evaluate its effects on EAE severity in infected mice.

Interestingly nematode infection induced a huge increased in the percentage of CD11b^{lo} peritoneal cavity cells that are F4/80$^-$, a typical phenotype for neutrophils (Matsushima et al., 2013). The result is particularly interesting as neutrophils play a substantial role in the pathogenesis of EAE (Wu et al., 2010). Circulating neutrophils are rapidly recruited to the sites of tissue damage, where they recruit monocytes and remodel damaged tissues; for these reasons, the implication that infection can change neutrophil phenotype and or/

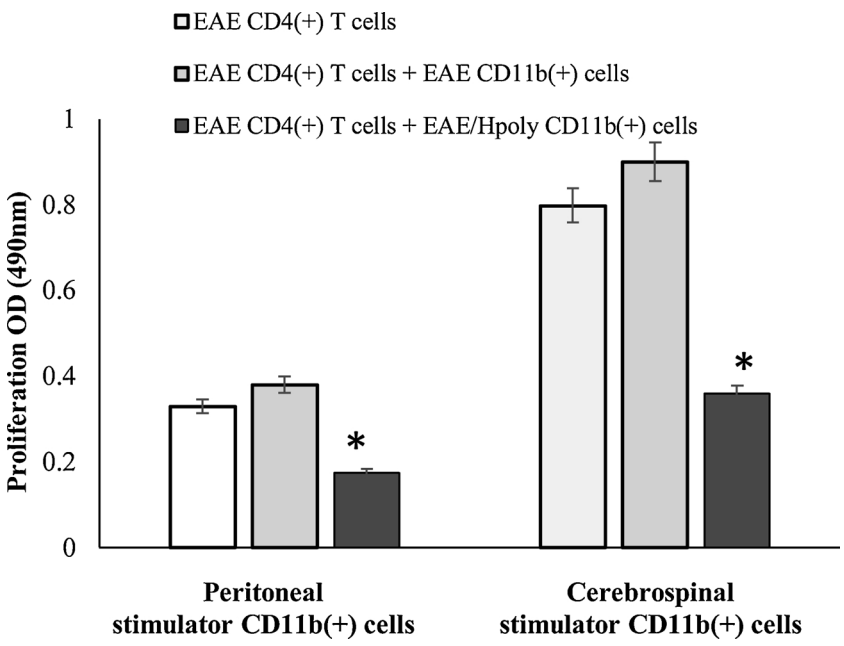

Fig. 5. MLR ability of $CD11b^+$ cells obtained from the CSF and PF of EAE mice uninfected (EAE) and infected with nematodes (EAE/Hpoly). $CD11b^+$ cells and $CD4^+$ T cells were isolated by negative selection using magnetic beads. Controls were set without $CD11b^+$ cells (EAE $CD4^+$ T cells). Specific proliferation was measured after 48 -h incubation with 5 μM of $MOG_{35–55}$ * indicates significant cell proliferation compared with EAE cells treated by the same manner, given as OD ± SD ($p < 0.05$).

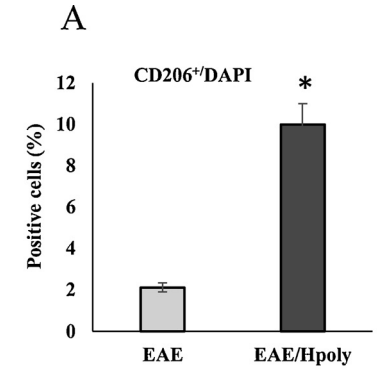

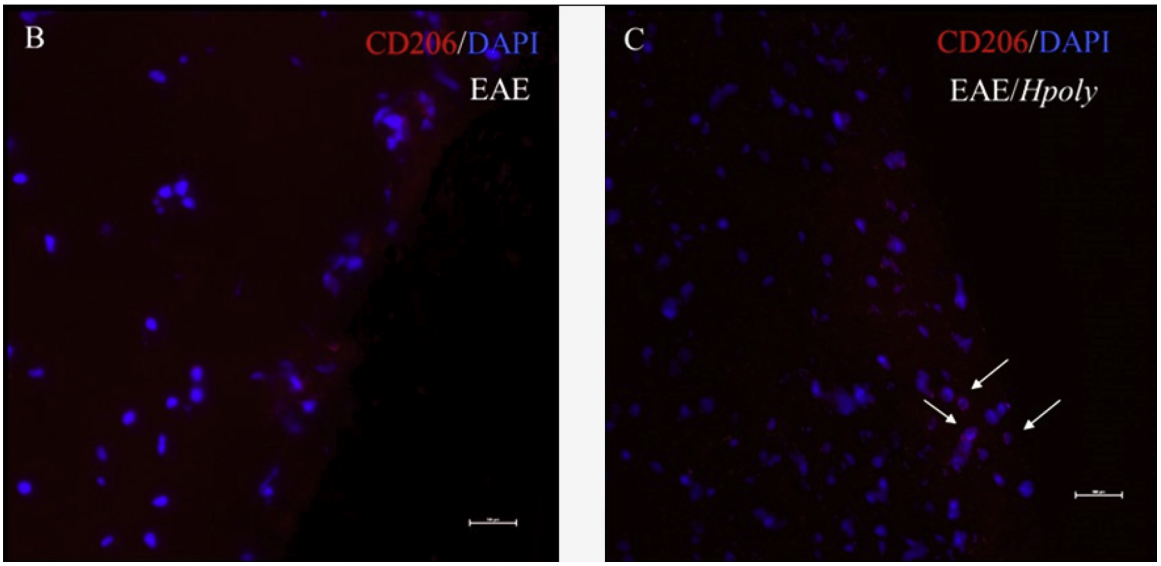

Fig. 6. $CD206^+/DAPI^+$ cells in EAE mice at six days post-infection with *H. polygyrus*. The nematode- treated EAE mice demonstrated higher numbers of CD206 expressing (red) DAPI(+) cells (blue) cells. The graphs represent the percentage of CD206(+)/DAPI(+) cells per DAPI(+) cells (A). Six random fields at 40x fields were counted for each mouse. Low-magnification image of cerebral cortex (Scale bar = 100 mm) highlighted by fluorescence imaging following staining with anti-CD206 mAb and DAPI: uninfected (B) and infected (C) EAE mice. Differences in immunostaining intensities and colours result from tissue destruction. The results of one representative experiment are presented as the mean ± SD of six mice. The relationship between groups was assessed by ANOVA. The results are presented as the mean values ± SD. *P < 0.05 compared to values obtained in EAE mice. (For interpretation of the references to colour in this figure legend, the reader is referred to the web version of this article).

infiltration in EAE merits further research.

On the other hand, our results indicate a rise in the number of CD11b cells expressing the F4/80 receptor and CD206 mannose receptor (MR) in the peritoneal cavity following infection. F4/80 possess anti-inflammatory, suppressive, tissue-repairing and anti-proliferative abilities, and are known to be associated with inhibition of the neuroinflammatory response (Schwartz and Baruch, 2014). Macrophages expressing F4/80 also manage the hyporesponsiveness of CD4-T cells and potently inhibit antigen-specific $CD4^+$ T-cell proliferative responses in the presence of competent naive APC (Taylor et al., 2006). Interestingly, in the CSF, the percentage of $F4/80^+$ cells expressing CD206 decreased after nematode infection, as did the percentage of $CD206^+$ cells expressing CD11b. Therefore, to identify the $CD206^+$ cells, the next part of our study evaluate the numbers of cells positive for CD206 and DAPI in mouse brain sections; brain tissue was chosen because the therapeutic effect in EAE is observed both in the brain and spinal cord (Sewell et al., 2003b). In contrast to the F4/80 receptors, no immunoreactivity was demonstrated for CD206 among microglia, but it was observed for macrophages (Peferoen et al., 2015). Numerous $CD206^+$/DAPI cells were localized in the sections taken from infected mice with EAE, and it appeared that nematode infection enhanced and restored the number of MMR^+ macrophages in EAE mice (unpublished observations). Although MMRs are known to recognize terminal mannose, N-acetylglucosamine and fucose residues on glycans attached to the proteins of pathogens (Schlesinger et al., 1978), little is understood of the activity of these receptors against nematode antigens (Hurst and Else, 2013; Blum et al., 2012). As increased CD11b expression is known to correspond to the severity of microglial activation in various neuroinflammatory diseases (Ling and Wong, 1993), further immunohistopathological studies using a combination of CD11b, CD45, CD206 labelling should be performed to distinguish microglia from leukocytes.

The $CD11b^+$ cells induced by the nematode demonstrated considerable heterogeneity, as indicated by their gene expression patterns. The peritoneal cavity $CD11b^+$ cells showed an expression profile closer to M2- than M1- type macrophages, i.e. an increase in Ym-1 and a decrease in Arg-1, as well as a decrease in iNOS and ROS; in contrast, the cerebrospinal CD11b cells were characterised by upregulation of Ym-1 and weak expression of Arg-1, iNOS-2 and ROS, which is typical for a mixture of classical and M2 phenotypes.

The metabolism of arginine is rerouted by M2 macrophages to produce ornithine and polyamine, thereby fostering cell growth and leading to tissue repair. However, in the sampled PF, NO was produced by both the CD11b cells exposed to LPS and those that were not; these findings indicate that iNOS activity is quickly exhausted in macrophages in the CNS following activation during EAE, most probably due to it being substituted by arginase. Arginase, a competitive enzyme of iNOS, then substitutes for the catalysis of L-arginine, resulting in lowered production of nitric oxide (Ahn et al., 2012).

This indicates that the peritoneal cavity, cells activated by nematode antigens are capable of carrying out processes involved in intracellular killing, a mechanism associated with classically-activated macrophages. Our results indicate that the peritoneal cavity contains proinflammatory M1-like phenotypes and anti-inflammatory or propreparative M2-like phenotypes, which are possibly responsible for facilitating tissue repair after L3 migration and L4 stage tissue localization; these are activated in response to high levels of TNF-α (unpublished data), which enhances the production of superoxide anions and NO (Hashimoto et al., 2013; Modolell et al., 1995).

However, the observation that macrophages display heterogeneity in terms of their function, and that their precise function is dependent on their anatomical location, is an important one. In the CNS, it has been postulated that the effects of classically-activated macrophages can be suppressed by astrocytes *via* TGF − β inhibition of NO production (Daley et al., 2010; Rogister et al., 1993). Such suppression may therefore take place in response to the high levels of TGF-β identified in EAE mice infected with *H. polygyrus* (Donskow-Łysoniewska et al., 2017). However, it cannot be excluded that microglial cells may serve as the major source of reactive nitrogen and oxygen species.

The observed differential accumulation of the two CD11b populations following nematode infection are in line with findings obtained by a study on *Schistosoma mansoni ova,* in which the percentage of CD11b cells that produced IL-12 was reduced, but that of those producing TNF remained unchanged (Sewell et al., 2003a). Changes in the surface expression of CD11b allow some speculation as to the differentiation pathways of $CD11b^+$ cells entering the CNS in response to infection. Based upon our data, it is possible that $CD11b^+$ cells located in the PF may be activated by infection and increase their expression of CD11b, becoming activated cells in the CNS. On the other hand, tissue-resident macrophages, such as brain macrophages, are independent of blood-derived macrophages as they are self-maintaining locally during adulthood (Modolell et al., 1995). However, during inflammation, their phenotype and activity can be influenced by the influx of blood-derived macrophages infiltrating the tissue, resulting in a mixture of resident and blood-derived macrophages (Yamasaki et al., 2014). However, it is not clear whether the infiltrating $CD11b^+$ cells in the CNS are derived from a subset of entirely newly-recruited cells, or are created by existing cells switching their phenotype during nematode infection. It has been postulated that the microenvironment within the CNS lesion does not allow local conversion of macrophages to an M2 phenotype, which is in line with the inability of activated resident microglia to attain a resolving phenotype at this critical stage (Shechter et al., 2009).

The infiltration of circulating monocytes after mechanical injury (e.g. nematode larvae passing through the intestine) and/or gut microbiota changes to the CNS has generally been attributed to mechanical damage to the parenchymal blood-brain barrier (BBB): blood-derived macrophages contribute to CNS repair, in part by displaying a resolving M2 phenotype (Schlesinger et al., 1978). This may well be the case, as the entry of cells into the CNS, indicated by high expression of CD11b, would satisfy the need for controlled recruitment of cells required for the inhibition of inflammation and/or repair; however, other mechanisms such as temporary BBB disruption by L4 stage nematode infection cannot be excluded. Nevertheless, future studies are planned to more precisely determine the regulatory role of these cells, including an analysis of neutrophil infiltration and activity, with the aim of clarifying the mechanisms involved in the inhibition of such pro-inflammatory responses.

Declaration of Competing Interest

The authors report no conflict of interest.

Acknowledgments

This work was supported by Grants for Scientific Research from the Polish National Science Centre (No. N303 819140 and No. 2014/15/N/NZ6/025025). We thank Katarzyna Kopec for technical assistance in writing the manuscript.

References

Huitinga, I., van Rooijen, N., de Groot, C.J., Uitdehaag, B.M., Dijkstra, C.D., 1990. Suppression of experimental allergic encephalomyelitis in Lewis rats after elimination of macrophages. J. Exp. Med. 172, 1025–1033. https://doi.org/10.1084/jem.172.4.1025.

Geurts, J.J., Barkhof, F., 2008. Grey matter pathology in multiple sclerosis. Lancet Neurol. 7, 841–851. https://doi.org/10.1016/S1474-4422(08)70191-1.

Kawakami, N., Lassmann, S., Li, Z., Odoardi, F., Ritter, T., Ziemssen, T., Klinkert, W.E., Ellwart, J.W., Bradl, M., Krivacic, K., et al., 2004. The activation status of neuroantigen-specific T cells in the target organ determines the clinical outcome of autoimmune encephalomyelitis. J. Exp. Med. 199, 185–197. https://doi.org/10.1084/jem.20031064.

Keating, P., O'Sullivan, D., Tierney, J.B., Kenwright, D., Miromoeini, S., Mawasse, L., Brombacher, F., La Flamme, A.C., 2009. Protection from EAE by IL-4Ralpha(−/−) macrophages depends upon T regulatory cell involvement. Immunol. Cell Biol. 87,

534–545. https://doi.org/10.1038/icb.2009.37.
Sewell, D., Qing, Z., Reinke, E., Elliot, D., Weinstock, J., Sandor, M., 2003a. Immunomodulation of experimental autoimmune encephalomyelitis by helminth ova immunization. Int. Immunol. 15, 59–69. https://doi.org/10.1093/intimm/dxg012.
La Flamme, A.C., Ruddenklau, K., Backstrom, B.T., 2003. Schistosomiasis decreases central nervous system inflammation and alters the progression of experimental autoimmune encephalomyelitis. Infect. Immun. 71, 4996–5004. https://doi.org/10.1128/IAI.71.9.4996-5004.2003.
Zheng, X., Hu, X., Zhou, G., Lu, Z., Qiu, W., Bao, J., Dai, Y., 2008. Soluble egg antigen from Schistosoma japonicum modulates the progression of chronic progressive experimental autoimmune encephalomyelitis via Th2-shift response. J. Neuroimmunol. 194, 107–114. https://doi.org/10.1016/j.jneuroim.2007.12.001.
Terrazas, C., de Dios Ruiz-Rosado, J., Amici, S.A., Jablonski, K.A., Martinez-Saucedo, D., Webb, L.M., Cortado, H., Robledo-Avila, F., Oghumu, S., Satoskar, A.R., Rodriguez-Sosa, M., Terrazas, L.I., Guerau-de Arellano, M., Partida-Sanchez, S., 2017. Helminth-induced ly6c hi monocyte-derived alternatively activated macrophages suppress experimental autoimmune encephalomyelitis. Sci. Rep. 7, 40814. https://doi.org/10.1038/srep40814.
Donskow-Łysoniewska, K., Krawczak, K., Bocian, K., Doligalska, M., 2017. The effects of intestinal nematode L4 stage on mouse experimental autoimmune encephalomyelitis. Arch. Immunol. Ther. Exp. 66, 231–243. https://doi.org/10.1007/s00005-017-0489-z.
Abram, C.L., Lowell, C.A., 2009. The ins and outs of leukocyte integrin signaling. Annu. Rev. Immunol. 27, 339–362. https://doi.org/10.1146/annurev.immunol.021908.132554.
Springer, T.A., Anderson, D.C., 1986. The importance of the Mac-1, LFA-1 glycoprotein family in monocyte and granulocyte adherence, chemotaxis, and migration into inflammatory sites: insights from an experiment of nature. Ciba Found. Symp. 118, 102–126.
Liu, L., Kubes, P., 2003. Molecular mechanisms of leukocyte recruitment: organ-specific mechanisms of action. J. Thromb. Haemost. 89, 213–220.
Bullard, D.C., Hu, X., Schoeb, T.R., Axtell, R.C., Raman, C., Barnum, S.R., 2005. Critical requirement of CD11b (Mac-1) on T cells and accessory cells for development of experimental autoimmune encephalomyelitis. J. Immunol. 175 (10), 6327–6333. https://doi.org/10.4049/jimmunol.175.10.6327.
Ehirchiou, D., Xiong, Y., Xu, G., Chen, W., Shi, Y., Zhang, L., 2007. CD11b facilitates the development of peripheral tolerance by suppressing Th17 differentiation. J. Exp. Med. 204 (7), 1519–1524. https://doi.org/10.1084/jem.20062292.
Donskow-Łysoniewska, K., Krawczak, K., Doligalska, M., 2012. Heligmosomoides polygyrus: EAE remission is correlated with different systemic cytokine profiles provoked by L4 and adult nematodes. Exp. Parasitol. 132, 243–248. https://doi.org/10.1016/j.exppara.2012.07.009.
Taylor, M.D., Harris, A., Nair, M.G., Maizels, R.M., Allen, J.E., 2006. F4/80^{+}alternatively activated macrophages control CD4^{+}T cell hyporesponsiveness at sites peripheral to filarial infection. J. Immunol. 176, 6918–6927. https://doi.org/10.4049/jimmunol.176.11.6918.
Ajami, B., Bennett, J.L., Krieger, C., Tetzlaff, W., Rossi, F.M.V., 2007. Local self-renewal can sustain CNS microglia maintenance and function throughout adult life. Nat. Neurosci. 10 (12), 1538–1543. https://doi.org/10.1038/nn2014.
Robbins, C.S., Hilgendorf, I., Weber, G.F., Theurl, I., Iwamoto, Y., Figueiredo, J.L., Gorbatov, R., Sukhova, G.K., Gerhardt, L.M., Smyth, D., Zavitz, C.C., Shikatani, E.A., Parsons, M., van Rooijen, N., Lin, H.Y., Husain, M., Libby, P., Nahrendorf, M., Weissleder, R., Swirski, F.K., 2013. Local proliferation dominates lesional macrophage accumulation in atherosclerosis. Nat. Med. 19 (9), 1166–1172. https://doi.org/10.1038/nm.3258.
Ghosn, E.E., Cassado, A.A., Govoni, G.R., Fukuhara, T., Yang, Y., Monack, D.M., Bortoluci, K.R., Almeida, S.R., Herzenberg, L.A., Herzenberg, L.A., 2010. Two physically, functionally, and developmentally distinct peritoneal macrophage subsets. Proc. Natl. Acad. Sci. U. S. A. 107, 2568–2573. https://doi.org/10.1073/pnas.0915000107.
Ponomarev, E.D., Shriver, L.P., Maresz, K., Dittel, B.N., 2005. Microglial cell activation and proliferation precedes the onset of CNS autoimmunity. J. Neurosci. Res. 81, 374–389. https://doi.org/10.1002/jnr.20488.
Renno, T., Lin, J.Y., Piccirillo, C., Antel, J., Owens, T., 1994. Cytokine production by cells in cerebrospinal fluid during experimental allergic encephalomyelitis in SJL/J mice. J. Neuroimmunol. 49 (1-2), 1–7. https://doi.org/10.1016/0165-5728(94)90174-0.
Matsushima, H., Geng, S., Lu, R., Okamoto, T., Yao, Y., Mayuzumi, N., Takashima, A., 2013. Neutrophil differentiation into a unique hybrid population exhibiting dual phenotype and functionality of neutrophils and dendritic cells. Blood 121 (10), 1677–1689. https://doi.org/10.1182/blood-2012-07-445189.
Dudhgaonkar, S.P., Janardhanam, S.B., Kodumudi, K.N., Srinivasan, M., 2009. CD80 blockade enhance glucocorticoid-induced leucine zipper expression and suppress experimental autoimmune encephalomyelitis. J. Immunol. 183, 7505–7513. https://doi.org/10.4049/jimmunol.0902056.
Girvin, A.M., Dal Canto, M.C., Miller, S.D., 2002. CD40/CD40L interaction is essential for the induction of EAE in the absence of CD28-mediated co-stimulation. J. Autoimmun. 18, 83–94. https://doi.org/10.1006/jaut.2001.0573.
Akbari, O., DeKruyff, R.H., Umetsu, D.T., 2001. Pulmonary dendritic cells producing IL-10 mediate tolerance induced by respiratory exposure to antigen. Nat. Immunol. 2, 725–731. https://doi.org/10.1038/90667.
Wu, F., Cao, W., Yang, Y., Liu, A., 2010. Extensive infiltration of neutrophils in the acute phase of experimental autoimmune encephalomyelitis in C57BL/6 mice. Histochem. Cell Biol. 133 (3), 313–322. https://doi.org/10.1007/s00418-009-0673-2.
Schwartz, M., Baruch, K., 2014. The resolution of neuroinflammation in neurodegeneration: leukocyte recruitment via the choroid plexus. EMBO J. 33, 7–22. https://doi.org/10.1002/embj.201386609.
Sewell, D., Qing, Z., Reinke, E., Elliot, D., Weinstock, J., Sandor, M., Fabry, Z., 2003b. Immunomodulation of experimental autoimmune encephalomyelitis by helminth ova immunization. Int. Immunol. 15, 59–69. https://doi.org/10.1093/intimm/dxg012.
Peferoen, L.A., Vogel, D.Y., Ummenthum, K., Breur, M., Heijnen, P.D., Gerritsen, W.H., Peferoen-Baert, R.M., van der Valk, P., Dijkatra, C.D., Amor, S., 2015. Activation status of human microglia is dependent on lesion formation stage and remyelination in multiple sclerosis. J. Neuropathol. Exp. Neurol. 74, 48–63. https://doi.org/10.1097/NEN.0000000000000149.
Schlesinger, P.H., Doebber, T.W., Mandell, B.F., White, R., DeSchryver, C., Rodman, J.S., Miller, M.J., Stahl, P., 1978. Plasma clearance of glycoproteins with terminal mannose and N-acetylglucosamine by liver non-parenchymal cells. Studies with beta-glucuronidase, N-acetyl-beta-D-glucosaminidase, ribonuclease B and agalacto-orosomucoid. Biochem. J. 176, 103–109. https://doi.org/10.1042/bj1760103.
Hurst, R.J., Else, K.J., 2013. The retinoic acid-producing capacity of gut dendritic cells and macrophages is reduced during persistent T. muris infection. Parasite Immunol. 35, 229–233. https://doi.org/10.1111/pim.12032.
Blum, A.M., Hang, L., Setiawan, T., Urban, J.P., Stoyanoff, K.M., Leung, J., Weinstock, J.V., 2012. Heligmosomoides polygyrus bakeri induces tolerogenic dendritic cells that block colitis and prevent antigen-specific gut T cell responses. J. Immunol. 189, 2512–2520. https://doi.org/10.4049/jimmunol.1102892.
Ling, E.A., Wong, W.C., 1993. The origin and nature of ramified and amoeboid microglia: a historical review and current concepts. Glia 7 (1), 9–18.
Ahn, M., Yang, W., Kim, H., Jin, J.K., Moon, C., Shin, T., 2012. Immunohistochemical study of arginase-1 in the spinal cords of Lewis rats with experimental autoimmune encephalomyelitis. Brain Res. 9 (1453), 77–86.
Hashimoto, D., Chow, A., Noizat, C., Teo, P., Beasley, M.B., Leboeuf, M., Becker, C.D., See, P., Price, J., Lucas, D., Greter, M., Mortha, A., Boyer, S.W., Forsberg, E.C., Tanaka, M., van Roojien, N., Garcia-Sastre, A., Stanley, R.E., Merad, M., 2013. Tissue-resident macrophages self-maintain locally throughout adult life with minimal contribution from circulating monocytes. Immunity 38, 792–804. https://doi.org/10.1016/j.immuni.2013.04.004.
Modolell, M., Corraliza, I.M., Link, F., Soler, G., Eichmann, K., 1995. Reciprocal regulation of the nitric oxide synthase/arginase balance in mouse bone marrow-derived macrophages by TH1 and TH2 cytokines. Eur. J. Immunol. 25, 1101–1104. https://doi.org/10.1002/eji.1830250436.
Daley, J.M., Brancato, S.K., Thomay, A.A., Reichner, J.S., Albina, J.E., 2010. The phenotype of murine wound macrophages. J. Leukoc. Biol. 87, 59–67. https://doi.org/10.1189/jlb.0409236.
Rogister, B., Delree, P., Leprince, P., Martin, D., Sadzot, C., Malgrange, B., Munaut, C., Rigo, J.M., Lefebvre, P.P., Octave, J.N., Schoenen, J., Moonen, G., 1993. Transforming growth factor β as a neuronoglial signal during peripheral nervous system response to injury. J. Neurosci. Res. 34, 32–43. https://doi.org/10.1002/jnr.490340105.
Yamasaki, R., Lu, H., Butovsky, O., Ohno, N., Rietsch, A.M., Cialic, R., Wu, P.M., Doykan, C.E., Lin, J., Cotleur, A.C., Kidd, G., Zorlu, M.M., Sun, N., Hu, W., Liu, L., Lee, J.C., Taylor, S.E., Uehlein, L., Dixon, D., Gu, J., Floruta, C.M., Zhu, M., Charo, I.F., Weiner, H.L., Ransohoff, R.M., 2014. Differential roles of microglia and monocytes in the inflamed central nervous system. J. Exp. Med. 211, 1533–1549. https://doi.org/10.1084/jem.20132477.
Shechter, R., London, A., Varol, C., Raposo, C., Cusimano, M., Yovel, G., Rolls, A., Mack, M., Pluchino, S., Martino, G., 2009. Infiltrating blood-derived macrophages are vital cells playing an anti-inflammatory role in recovery from spinal cord injury in mice. PLoS Med. 6, e1000113. https://doi.org/10.1371/journal.pmed.1000113.